



# Conforming $P_3$ Divergence-Free Finite Elements for the Stokes Equations on Subquadrilateral Triangular Meshes

Shangyou Zhang<sup>1</sup>

*In Honor of the Memory of Professor Zhong-Ci Shi.*

Received: 3 March 2023 / Revised: 2 August 2023 / Accepted: 3 October 2023  
© Shanghai University 2023

## Abstract

The continuous  $P_3$  and discontinuous  $P_2$  finite element pair is stable on subquadrilateral triangular meshes for solving 2D stationary Stokes equations. By putting two diagonal lines into every quadrilateral of a quadrilateral mesh, we get a subquadrilateral triangular mesh. Such a velocity solution is divergence-free point wise and viscosity robust in the sense the solution and the error are independent of the viscosity. Numerical examples show an advantage of such a method over the Taylor-Hood  $P_3$ - $P_2$  method, where the latter deteriorates when the viscosity becomes small.

**Keywords** Divergence-free · Stokes equations · Finite element · Triangular mesh · Quadrilateral mesh

**Mathematics Subject Classification** 65N15 · 65N30

## 1 Introduction

We solve a model Stokes problem,

$$\begin{aligned} -\mu\Delta\mathbf{u} + \nabla p &= \mathbf{f} \quad \text{in } \Omega, \\ \mathbf{u} &= \mathbf{0} \quad \text{on } \partial\Omega, \end{aligned}$$

where  $\mu > 0$  is the viscosity and  $\Omega$  is bounded polygonal domain in 2D. The weak form is: find  $(\mathbf{u}, p) \in H_0^1(\Omega) \times L_0^2(\Omega)$  such that

$$(\mu\nabla\mathbf{u}, \nabla\mathbf{v}) - (p, \operatorname{div}\mathbf{v}) = (\mathbf{f}, \mathbf{v}), \quad \forall \mathbf{v} \in H_0^1(\Omega), \quad (1)$$

---

✉ Shangyou Zhang  
szhang@udel.edu

<sup>1</sup> Department of Mathematical Sciences, University of Delaware, Newark, DE 19716, USA

$$(q, \operatorname{div} \mathbf{u}) = 0, \quad \forall q \in L_0^2(\Omega). \quad (2)$$

A natural finite element method for the Stokes equations would be the  $P_k$ - $P_{k-1}$  element on triangular and tetrahedral grids which approximates the velocity in an  $H^1$ -subspace  $\mathbf{V}_h$  of continuous  $P_k$  functions (referred as  $C^0$ - $P_k$ ), and approximates the pressure in an  $L^2$ -subspace  $P_h$  of discontinuous  $P_{k-1}$  functions (referred as  $C^{-1}$ - $P_{k-1}$ ). In this case, the finite element problem reads: find  $(\mathbf{u}_h, p_h) \in \mathbf{V}_h \times P_h \subset H_0^1(\Omega) \times L_0^2(\Omega)$  such that

$$(\mu \nabla \mathbf{u}_h, \nabla \mathbf{v}_h) - (p_h, \operatorname{div} \mathbf{v}_h) = (\mathbf{f}, \mathbf{v}_h), \quad \forall \mathbf{v}_h \in \mathbf{V}_h, \quad (3)$$

$$(q_h, \operatorname{div} \mathbf{u}_h) = 0, \quad \forall q_h \in P_h. \quad (4)$$

In this case the divergence-free condition is satisfied point wise and the discrete solution for the velocity is the Galerkin projection within the space of divergence-free functions. Therefore the numerical solution  $\mathbf{u}_h$  is independent of  $p$  and its error is independent of the viscosity  $\mu$ . But other methods, for example, the Taylor-Hood finite element, would deteriorate when  $\mu$  is small. However, the  $P_k$ - $P_{k-1}$  method is not stable in general. Scott and Vogelius showed in [16, 17] that the method is stable and consequently of the optimal order on 2D triangular grids for polynomial degree  $k \geq 4$ , provided the grids have no nearly-singular vertex. Many works on the divergence-free  $P_k$ - $P_{k-1}$  finite element method have been done, mostly on macro-type meshes or with bubble stabilization, cf. [1–15, 19–26].

The  $P_3$ - $P_2$  finite element is not stable. In [4], it is stabilized by enriching  $P_3$  space with some rational, divergence-free bubbles. In Zhang- $P_3$ , it is stabilized by enriching  $P_3$  space with some  $P_4$  divergence-free bubbles. Computationally, these methods solved the problem. Mathematically, one would like to know if the method can be stable without adding bubbles in some cases. If so, the method would be more efficient in computation without bubbles.

The  $P_3$ - $P_2$  finite element is not stable on general triangular meshes. In this work, we show the element is stable on subquadrilateral triangular meshes. What is a subquadrilateral triangular mesh? After we put two diagonal lines into every quadrilateral in a quadrilateral mesh, we get a subquadrilateral triangular mesh. We can also obtain such a mesh from a quasi-uniform triangular mesh of even number of triangles, see Fig. 1. We simply connect the two opposite points on two sides of an edge which is shared by a pair of triangles, see Fig. 1b. In both cases, the intersection point is a singular vertex, in terms of finite element analysis. At a singular vertex, the discrete pressure function is not a totally discontinuous  $P_2$  function. The four values of a discrete pressure  $p_2(\mathbf{x})$  are subject to a continuity condition that  $\sum_{i=1}^4 (-1)^i p_2|_{T_i}(\mathbf{n}_0) = 0$ ,

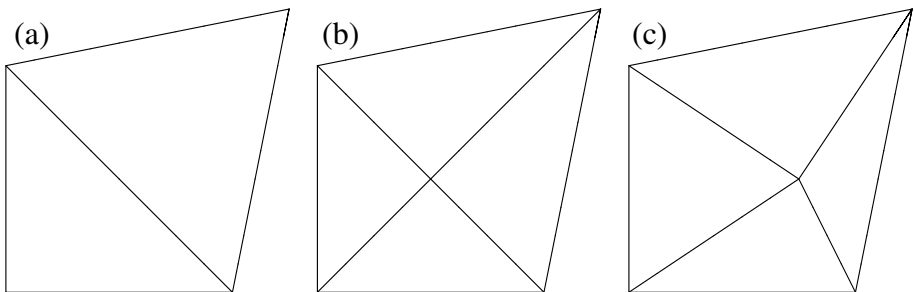


**Fig. 1** a Two triangles in a triangular mesh form a quadrilateral. b A subquadrilateral triangular mesh. c A subquadrilateral triangular mesh without any singular vertex

where  $\mathbf{n}_0$  is the intersection point. A singular vertex would cause some extra work in computer coding. To avoid a singular vertex in this case, one can move the center point to any point of distance  $Ch$  away for some fixed  $C > 0$ , see Fig. 1c. If it is moved a way by a distance, say  $h^2$ , we would have a nearly singular vertex. Then the method is no longer stable. Though a singular vertex creates more coding work, the method would be more accurate and be more efficient with less degrees of freedom. We limit this work on the case with a singular vertex. Numerical tests are presented confirming the theory. Numerical comparison also shows the robustness of the method when  $\mu \ll 1$ , and its advantage over the Taylor-Hood  $P_3$ - $P_2$  method.

Because the method is divergence-free, its pressure error is usually 100 times larger than that of the  $P_3$ - $P_2$  Taylor-Hood element. However, for large Reynolds number flows, this method would be a Reynolds number times better, e.g., both pressure and velocity errors are  $10^6$  times less than that of the other method, cf. Tables 2 and 4. One would expect that it is more efficient numerically if one subdivides a quadrilateral into two triangles instead of four. But if we view the grid at a  $45^\circ$  rotation, we would realize this 4-triangle subdivision is exactly a 2-triangle subdivision on size  $h/\sqrt{2}$  quadrilaterals. Thus the two subdivisions are equally efficient.

### 2 Inf-sup Stability

Let  $\mathcal{Q}_h = \{Q\}$  be a quasi-uniform quadrilateral mesh on the domain  $\Omega$ , where  $h = \max\{\text{diameter}(Q)\}$ . Connecting two pairs of points on each quadrilateral  $Q (= \cup_{i=1}^4 T_i)$ , we obtain a quasi-uniform triangular mesh  $\mathcal{T}_h = \{T_i\}$ , see Fig. 2.

The velocity finite element space is defined by

$$\mathbf{V}_h = \{ \mathbf{v}_h \in H_0^1(\Omega)^2 : \mathbf{v}_h|_{T_i} \in P_3(T_i)^2, T_i \in \mathcal{T}_h \}. \tag{5}$$

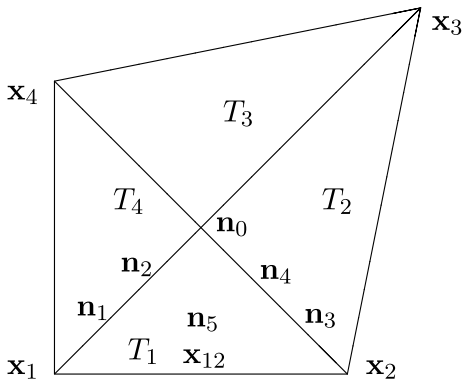
The pressure finite element space is defined by

$$P_h = \left\{ p_h \in L_0^2(\Omega) : p_h|_{T_i} \in P_2, \sum_{i=1}^4 (-1)^i p_h|_{T_i}(\mathbf{n}_0) = 0 \right\}, \tag{6}$$

where  $\mathbf{n}_0$  is the intersection point of two diagonals of quadrilateral  $Q = \cup_{i=1}^4 T_i$ .

**Lemma 1** *Let  $p_2 \in P_h$  defined in (6). There is a  $\mathbf{u}_h \in \mathbf{V}_h$ , defined in (5), such that*

Fig. 2 Lagrange nodes on  $T_1$



$$\operatorname{div} \mathbf{u}_h = p_2 \quad \text{and} \quad |\mathbf{u}_h|_1 \leq C \|p_2\|_0. \tag{7}$$

Consequently,

$$\beta \leq \inf_{p_h \in P_h} \sup_{\mathbf{v}_h \in \mathbf{V}_h} \frac{(\operatorname{div} \mathbf{v}_h, p_h)}{|\mathbf{v}_h|_1 \|p_h\|_0}, \tag{8}$$

where  $\beta > 0$  is independent of the mesh size  $h$ .

**Proof** Let  $p_2 \in P_h$ . There is a smooth function  $\mathbf{u} \in H_0^1(\Omega)^2 \cap H^2(\Omega)^2$  such that

$$\operatorname{div} \mathbf{u} = p_2 \quad \text{and} \quad |\mathbf{u}|_1 \leq C \|p_2\|_0.$$

We do a modified Lagrange interpolation  $\mathbf{u}_{h,1}$  of  $\mathbf{u}$ . Except one node each edge, we interpolate  $\mathbf{u}_{h,1}(\mathbf{n}_i) = \mathbf{u}(\mathbf{n}_i)$  at the rest nodes. At the special mid-edge nodes,  $\mathbf{u}_{h,1}(\mathbf{n}_i)$  are chosen such that

$$\int_{\mathbf{x}_1 \mathbf{n}_0} (\mathbf{u}_{h,1} - \mathbf{u}) \cdot \mathbf{n} \, ds = 0,$$

where  $\mathbf{n}$  is a normal vector on edge  $\mathbf{x}_1 \mathbf{n}_0$ , see Fig. 2. Let

$$p_{2,1} = p_2 - \operatorname{div} \mathbf{u}_{h,1} \in P_h. \tag{9}$$

Then we have, for all  $T_i \in \mathcal{T}_h$ ,

$$\int_{T_i} p_{2,1} \, d\mathbf{x} = \int_{T_i} (\operatorname{div} \mathbf{u} - \operatorname{div} \mathbf{u}_{h,1}) \, d\mathbf{x} = \int_{\partial T_i} (\mathbf{u} - \mathbf{u}_{h,1}) \cdot \mathbf{m}_i \, ds = 0, \tag{10}$$

where  $\mathbf{m}_i$  is the outward normal vector of  $T_i$ .

We will match  $p_{2,1}$  separately by constructing a  $\mathbf{u}_h \in H_0^1(Q)^2 \cap \mathbf{V}_h$ , on each patch of four triangles  $Q = \cup_{i=1}^4 T_i$ , cf. Fig. 2.

Such a  $\mathbf{u}_h$ , as  $\mathbf{u}_h|_{\mathbf{x}_1 \mathbf{x}_2} = \mathbf{0}$ , has the following expansion under the Lagrange basis that

$$\mathbf{u}_h|_{T_i} = \sum_{i=0}^5 \mathbf{u}_h(\mathbf{n}_i) \phi_i(\mathbf{x}). \tag{11}$$

We replace the degree of freedom (DOF) of  $P_3$  basis function of nodal value at  $\mathbf{n}_1$ , cf. Fig. 2, by the tangential derivative basis function at point  $\mathbf{x}_1$ . We do same replacement for Lagrange  $\mathbf{n}_3$  node. That is,

$$\begin{cases} \partial_{\mathbf{x}_1 \mathbf{n}_0} \phi_1(\mathbf{x}_1) = 1, & \partial_{\mathbf{x}_2 \mathbf{n}_0} \phi_1(\mathbf{x}_2) = 0, \\ \partial_{\mathbf{x}_1 \mathbf{n}_0} \phi_3(\mathbf{x}_1) = 0, & \partial_{\mathbf{x}_2 \mathbf{n}_0} \phi_3(\mathbf{x}_2) = 1, \\ \partial_{\mathbf{x}_1 \mathbf{n}_0} \phi_2(\mathbf{x}_1) = 0, & \partial_{\mathbf{x}_2 \mathbf{n}_0} \phi_2(\mathbf{x}_2) = 0. \end{cases} \tag{12}$$

Let

$$B = (\mathbf{x}_2 - \mathbf{x}_1 \quad \mathbf{n}_0 - \mathbf{x}_1), \quad \begin{pmatrix} b_{11} & b_{12} \\ b_{21} & b_{22} \end{pmatrix} = B^{-T}.$$

Then

$$\begin{aligned} \operatorname{div} \mathbf{u}_h|_{T_1}(\mathbf{x}_1) &= \partial_x(\mathbf{u}_h)_1 + \partial_y(\mathbf{u}_h)_2 \\ &= b_{11}\partial_{\mathbf{x}_1\mathbf{x}_2}(\mathbf{u}_h)_1 + b_{12}\partial_{\mathbf{x}_1\mathbf{n}_0}(\mathbf{u}_h)_1 \\ &\quad + b_{21}\partial_{\mathbf{x}_1\mathbf{x}_2}(\mathbf{u}_h)_2 + b_{22}\partial_{\mathbf{x}_1\mathbf{n}_0}(\mathbf{u}_h)_2 \\ &= b_{12}\partial_{\mathbf{x}_1\mathbf{n}_0}(\mathbf{u}_h)_1 + b_{22}\partial_{\mathbf{x}_1\mathbf{n}_0}(\mathbf{u}_h)_2 \\ &= \mathbf{b}_2 \cdot \partial_{\mathbf{x}_1\mathbf{n}_0} \mathbf{u}_h|_{T_1}(\mathbf{x}_1), \end{aligned}$$

where  $\mathbf{b}_2 = \langle b_{12}, b_{22} \rangle$ . Similarly, on  $T_4$ ,

$$\begin{aligned} \operatorname{div} \mathbf{u}_h|_{T_4}(\mathbf{x}_1) &= \partial_x(\mathbf{u}_h)_1 + \partial_y(\mathbf{u}_h)_2 \\ &= c_{11}\partial_{\mathbf{x}_1\mathbf{x}_2}(\mathbf{u}_h)_1 + c_{12}\partial_{\mathbf{x}_1\mathbf{n}_0}(\mathbf{u}_h)_1 \\ &\quad + c_{21}\partial_{\mathbf{x}_1\mathbf{x}_2}(\mathbf{u}_h)_2 + c_{22}\partial_{\mathbf{x}_1\mathbf{n}_0}(\mathbf{u}_h)_2 \\ &= c_{12}\partial_{\mathbf{x}_1\mathbf{n}_0}(\mathbf{u}_h)_1 + c_{22}\partial_{\mathbf{x}_1\mathbf{n}_0}(\mathbf{u}_h)_2 \\ &= \mathbf{c}_2 \cdot \partial_{\mathbf{x}_1\mathbf{n}_0} \mathbf{u}_h|_{T_4}(\mathbf{x}_1), \end{aligned}$$

where  $\mathbf{c}_2 = \langle c_{12}, c_{22} \rangle$ , and

$$C = (\mathbf{x}_4 - \mathbf{x}_1 \quad \mathbf{n}_0 - \mathbf{x}_1), \quad \begin{pmatrix} c_{11} & c_{12} \\ c_{21} & c_{22} \end{pmatrix} = C^{-T}.$$

Together, we have a linear system of two equations,

$$\begin{cases} \mathbf{b}_2 \cdot \partial_{\mathbf{x}_1\mathbf{n}_0} \mathbf{u}_h(\mathbf{x}_1) = p_2|_{T_1}(\mathbf{x}_1), \\ \mathbf{c}_2 \cdot \partial_{\mathbf{x}_1\mathbf{n}_0} \mathbf{u}_h(\mathbf{x}_1) = p_2|_{T_4}(\mathbf{x}_1). \end{cases} \tag{13}$$

Because  $\mathbf{b}_2 \perp \mathbf{x}_1\mathbf{x}_2$ ,  $\mathbf{c}_2 \perp \mathbf{x}_1\mathbf{x}_4$ ,  $\mathbf{x}_1\mathbf{x}_2$  and  $\mathbf{x}_1\mathbf{x}_4$  are not on a same line, and  $\mathbf{b}_2 \nparallel \mathbf{c}_2$ , (13) has a unique solution  $\partial_{\mathbf{x}_1\mathbf{n}_0} \mathbf{u}_h(\mathbf{x}_1)$ . Similarly we can find  $\partial_{\mathbf{x}_i\mathbf{n}_0} \mathbf{u}_h(\mathbf{x}_i)$ ,  $i = 1, \dots, 4$ , to match the two  $p_2$  values on two sides of the vertex.

Let  $\mathbf{u}_{h,2}$  be the  $\mathbf{V}_h$  function which has only the terms with  $\partial_{\mathbf{x}_i\mathbf{n}_0} \mathbf{u}_h(\mathbf{x}_i)$  (while the rest coefficients are zero under its modified Lagrange basis expansion (11).) Then we add it the other mid-edge nodal value functions  $(\mathbf{u}_h(\mathbf{n}_2)\phi_2$  and  $\mathbf{u}_h(\mathbf{n}_4)\phi_4$  on  $T_1$ ), which cancel the non-zero flux so that the new  $\mathbf{u}_{h,2}$  satisfies

$$\int_{\mathbf{x}_i\mathbf{n}_0} \mathbf{u}_{h,2} \cdot \mathbf{m}_i ds = 0$$

on the four internal edges. Let

$$p_{2,2} = p_{2,1} - \operatorname{div} \mathbf{u}_{h,2} \in L^2_0(Q) \cap \prod_{i=1}^4 P_2(T_i).$$

Then,  $p_{2,2}$  also satisfies (10) and vanishes at the corner vertexes,

$$p_{2,2}|_{T_j}(\mathbf{x}_j) = 0, \quad j = 1, \dots, 4 \tag{14}$$

for appropriate triangles.

We continue to match  $p_{2,2}$  by  $\operatorname{div} \mathbf{u}_{h,3}$  and more functions without destroying earlier matches. Such a  $\operatorname{div} \mathbf{u}_{h,3}$  must have the following expansion ( $\phi_i$  is no longer the standard Lagrange basis function but the modified one satisfying (12)):

$$\mathbf{u}_h|_{T_1} = \mathbf{u}_h(\mathbf{n}_0)\phi_0 + \mathbf{u}_h(\mathbf{n}_2)\phi_2 + \mathbf{u}_h(\mathbf{n}_4)\phi_4 + \partial_{\mathbf{x}_{12}\mathbf{n}_0} \mathbf{u}_h(\mathbf{x}_{12})\phi_5, \tag{15}$$

where  $\mathbf{x}_{12}$  is the middle point on the edge  $\mathbf{x}_1\mathbf{x}_2$ , cf. Fig. 2. In particular, we select only one term to construct  $\mathbf{u}_{h,3}$ ,

$$\mathbf{u}_h|_{T_1} = \partial_{\mathbf{x}_{12}\mathbf{n}_0} \mathbf{u}_h(\mathbf{x}_{12})\phi_5,$$

where  $\partial_{\mathbf{x}_{12}\mathbf{n}_0} \phi_5(\mathbf{x}_{12}) = 1$ . On  $T_1$ , we have

$$\begin{aligned} \operatorname{div} \mathbf{u}_h(\mathbf{x}_{12}) &= \partial_x(\mathbf{u}_h)_1 + \partial_y(\mathbf{u}_h)_2 \\ &= d_{11}\partial_{\mathbf{x}_{12}\mathbf{x}_2}(\mathbf{u}_h)_1 + d_{12}\partial_{\mathbf{x}_{12}\mathbf{n}_0}(\mathbf{u}_h)_1 \\ &\quad + d_{21}\partial_{\mathbf{x}_{12}\mathbf{x}_2}(\mathbf{u}_h)_2 + d_{22}\partial_{\mathbf{x}_{12}\mathbf{n}_0}(\mathbf{u}_h)_2 \\ &= d_{12}\partial_{\mathbf{x}_{12}\mathbf{n}_0}(\mathbf{u}_h)_1 + d_{22}\partial_{\mathbf{x}_{12}\mathbf{n}_0}(\mathbf{u}_h)_2 \\ &= \mathbf{d}_2 \cdot \partial_{\mathbf{x}_{12}\mathbf{n}_0} \mathbf{u}_h(\mathbf{x}_{12}), \end{aligned}$$

where  $\mathbf{d}_2 = \langle d_{12}, d_{22} \rangle$ , and

$$D = (\mathbf{x}_2 - \mathbf{x}_{12} \quad \mathbf{n}_0 - \mathbf{x}_{12}), \quad \begin{pmatrix} d_{11} & d_{12} \\ d_{21} & d_{22} \end{pmatrix} = D^{-\top}.$$

The second equation matches the divergence at another mid-edge point of  $T_1$ ,

$$\begin{aligned} \operatorname{div} \mathbf{u}_h(\mathbf{x}_{10}) &= \partial_x(\mathbf{u}_h)_1 + \partial_y(\mathbf{u}_h)_2 \\ &= c_{11}\partial_{\mathbf{x}_{10}\mathbf{x}_{20}}(\mathbf{u}_h)_1 + c_{12}\partial_{\mathbf{x}_{10}\mathbf{n}_0}(\mathbf{u}_h)_1 \\ &\quad + c_{21}\partial_{\mathbf{x}_{10}\mathbf{x}_{20}}(\mathbf{u}_h)_2 + c_{22}\partial_{\mathbf{x}_{10}\mathbf{n}_0}(\mathbf{u}_h)_2 \\ &= c_{12}\partial_{\mathbf{x}_{10}\mathbf{n}_0}(\mathbf{u}_h)_1 + c_{22}\partial_{\mathbf{x}_{10}\mathbf{n}_0}(\mathbf{u}_h)_2 \\ &= c_0\mathbf{c}_2 \cdot \partial_{\mathbf{x}_{12}\mathbf{n}_0} \mathbf{u}_h(\mathbf{x}_{12}), \end{aligned}$$

where  $\mathbf{x}_{10} = (\mathbf{x}_1 + \mathbf{n}_0)/2$  is the mid-point,  $\mathbf{x}_{20} = (\mathbf{x}_2 + \mathbf{n}_0)/2$ ,  $c_0 = \partial_{\mathbf{x}_{10}\mathbf{x}_{20}} \phi_5 > 0$ ,  $\mathbf{c}_2 = \langle c_{12}, c_{22} \rangle$ , and

$$C = (\mathbf{x}_{20} - \mathbf{x}_{10} \quad \mathbf{n}_0 - \mathbf{x}_{10}), \quad \begin{pmatrix} c_{11} & c_{12} \\ c_{21} & c_{22} \end{pmatrix} = C^{-\top}.$$

We have following two equations:

$$\begin{cases} \mathbf{d}_2 \cdot \partial_{\mathbf{x}_{12}\mathbf{n}_0} \mathbf{u}_h(\mathbf{x}_{12}) = p_{2,2}(\mathbf{x}_{12}), \\ c_0\mathbf{c}_2 \cdot \partial_{\mathbf{x}_{12}\mathbf{n}_0} \mathbf{u}_h(\mathbf{x}_{12}) = \frac{1}{2}(p_{2,2}(\mathbf{x}_{10}) - p_{2,2}(\mathbf{x}_{20})). \end{cases} \tag{16}$$

Because  $\mathbf{d}_2 \perp \mathbf{x}_{12}\mathbf{x}_2$ ,  $\mathbf{c}_2 \perp \mathbf{x}_1\mathbf{x}_2$ , and  $\mathbf{d}_2 \nparallel \mathbf{c}_2$ , (16) has a unique solution  $\partial_{\mathbf{x}_{12}\mathbf{n}_0} \mathbf{u}_h(\mathbf{x}_{12})$ . Let  $\mathbf{u}_{h,3}|_{T_1} = \partial_{\mathbf{x}_{12}\mathbf{n}_0} \mathbf{u}_h(\mathbf{x}_{12})\phi_5$  and

$$p_{2,3}|_{T_1} = p_{2,2} - \operatorname{div} \mathbf{u}_{h,3}.$$

Then

$$p_{2,3}|_{T_1} = p_{2,3}(\mathbf{n}_0)l_{\mathbf{n}_0} + p_{2,3}(\mathbf{x}_{10})(l_{\mathbf{x}_{10}} + l_{\mathbf{x}_{20}}),$$

where  $l_*$  is the Lagrange basis function at a  $P_2$  node, and

$$p_{2,3}(\mathbf{x}_{10}) = p_{2,3}(\mathbf{x}_{20}) = \frac{1}{2}(p_{2,2}(\mathbf{x}_{10}) + p_{2,2}(\mathbf{x}_{20}))$$

by the construction (16) and a symmetric divergence of  $\mathbf{c}\phi_5$ .  $p_{2,3}|_{T_1}$  has three non-zero nodal values. We will show it in fact has only one non-zero coefficient by the zero integral condition (10). That is,

$$\begin{aligned} 0 &= \int_{T_1} p_{2,3} \, d\mathbf{x} \\ &= p_{2,3}(\mathbf{n}_0) \int_{T_1} l_{\mathbf{n}_0} \, d\mathbf{x} + p_{2,3}(\mathbf{x}_{10}) \left( \int_{T_1} l_{\mathbf{x}_{10}} \, d\mathbf{x} + \int_{T_1} l_{\mathbf{x}_{20}} \, d\mathbf{x} \right) \\ &= 0 + p_{2,3}(\mathbf{x}_{10}) \left( \frac{1}{6}|T_1| + \frac{1}{6}|T_1| \right). \end{aligned}$$

Thus  $p_{2,3}(\mathbf{x}_{10}) = 0$  and

$$p_{2,3}|_{T_1} = p_{2,3}(\mathbf{n}_0)l_{\mathbf{n}_0}.$$

Defining  $\mathbf{u}_{h,3}$  on the other three triangles as we did on  $T_1$ , we let

$$p_{2,3} = p_{2,2} - \operatorname{div} \mathbf{u}_{h,3} \in L_0^2(Q) \cap P_h. \tag{17}$$

Then,  $p_{2,3}$  also satisfies (10) and (14), and vanishes at 4 outside mid-edge points and 8 mid-edge points,

$$p_{2,3}|_{T_i}(\mathbf{x}_{i,i+1}) = 0, \quad i = 1, \dots, 4, \tag{18}$$

$$p_{2,3}|_{T_i}(\mathbf{x}_{i,0}) = p_{2,3}|_{T_{i+1}}(\mathbf{x}_{i,0}) = 0, \quad i = 1, \dots, 4, \tag{19}$$

where we use a notation convention that  $\mathbf{x}_5 = \mathbf{x}_1$  and  $T_5 = T_1$ . We note that to get (19), we do not use/limit the DOF of  $\partial_{\mathbf{x},\mathbf{n}_0} \phi_1(\mathbf{x}_{10})$  and  $\partial_{\mathbf{x}_{10},\mathbf{x}_{20}} \phi_i(\mathbf{x}_{10})$  there. Thus in future construction, (19) is not preserved automatically, but (14) and (18) are.

The  $p_{2,3}$  in (17) has only 4 nodal values at the central point to be matched. We match  $p_{2,3}|_{T_1}(\mathbf{n}_0)$  next by a  $\operatorname{div} \mathbf{u}_h$ . On  $T_1$  and  $T_2$ , let

$$\mathbf{u}_h = \begin{cases} \mathbf{d}_1 \phi_4 & \text{on } T_1, \\ \mathbf{d}_1 \phi_2 & \text{on } T_2, \end{cases}$$

where  $\phi_i$  on different triangles are defined as in (15) and  $\mathbf{d}_1$  is determined by these two equations,

$$\operatorname{div} \mathbf{u}_h|_{T_1}(\mathbf{n}_0) = 1, \quad \int_{\mathbf{x}_2, \mathbf{n}_0} \mathbf{u}_h \cdot \mathbf{n} \, ds = 0. \tag{20}$$

For the first equation, we have

$$\begin{aligned} \operatorname{div} \mathbf{u}_h|_{T_1}(\mathbf{n}_0) &= \partial_x(\mathbf{u}_h)_1 + \partial_y(\mathbf{u}_h)_2 \\ &= c_{11}\partial_{\mathbf{n}_0\mathbf{x}_1}(\mathbf{u}_h)_1 + c_{12}\partial_{\mathbf{n}_0\mathbf{x}_2}(\mathbf{u}_h)_1 \\ &\quad + c_{21}\partial_{\mathbf{n}_0\mathbf{x}_1}(\mathbf{u}_h)_2 + c_{22}\partial_{\mathbf{n}_0\mathbf{x}_2}(\mathbf{u}_h)_2 \\ &= c_{12}(\mathbf{d}_1)_1/(-4) + c_{22}(\mathbf{d}_1)_2/(-4) \\ &= -\frac{1}{4}\mathbf{c}_2 \cdot \mathbf{d}_1, \end{aligned}$$

where  $\mathbf{c}_2 = \langle c_{12}, c_{22} \rangle$ , and

$$C = (\mathbf{x}_1 - \mathbf{n}_0 \quad \mathbf{x}_2 - \mathbf{n}_0), \quad \begin{pmatrix} c_{11} & c_{12} \\ c_{21} & c_{22} \end{pmatrix} = C^{-\top}.$$

For the second equation, we have

$$\int_{\mathbf{x}_2\mathbf{n}_0} \mathbf{u}_h \cdot \mathbf{n} ds = \left( \frac{2}{15} |\mathbf{x}_2\mathbf{n}_0| \right) \mathbf{n} \cdot \mathbf{d}_1.$$

As  $\mathbf{c}_2 \perp \mathbf{x}_1\mathbf{n}_0$ ,  $\mathbf{n} \perp \mathbf{x}_2\mathbf{n}_0$ , and  $\mathbf{c}_2 \nparallel \mathbf{n}$ , (20) has a unique solution  $\mathbf{d}_1$ . With it, we define

$$\mathbf{u}_{h,4} = \begin{cases} \mathbf{d}_1\phi_4 + \frac{1}{4}\mathbf{u}_1 & \text{on } T_1, \\ \mathbf{d}_1\phi_2 - \frac{1}{4}\mathbf{u}_2 & \text{on } T_2, \end{cases} \tag{21}$$

where  $\mathbf{d}_1$  is defined by (13) and  $\mathbf{u}_i$  is defined to be the solution of (16) with the right-hand side vector  $\langle 0, 1 \rangle$ ,

$$\mathbf{u}_i|_{T_i} = \mathbf{c}_i\phi_5, \quad i = 1, \dots, 4.$$

Here the function  $\mathbf{u}_1$  corrects  $\operatorname{div}(\mathbf{d}_1\phi_4)$  at the two mid-edge points  $\mathbf{x}_{10}$  and  $\mathbf{x}_{20}$ . Define

$$p_{2,4} = p_{2,3} - \operatorname{div} \mathbf{u}_{h,4} \in L_0^2(Q) \cap P_h.$$

We have

$$\begin{aligned} p_{2,4}|_{T_1}(\mathbf{y}) &= 0, \quad \mathbf{y} = \mathbf{x}_1, \mathbf{x}_{12}, \mathbf{x}_2, \mathbf{x}_{20}, \mathbf{n}_0, \mathbf{x}_{10}, \\ p_{2,4}|_{T_2}(\mathbf{n}_0) &= p_{2,3}|_{T_2}(\mathbf{n}_0) - p_{2,3}|_{T_1}(\mathbf{n}_0), \\ p_{2,4}|_{T_2}(\mathbf{y}) &= 0, \quad \mathbf{y} = \mathbf{x}_2, \mathbf{x}_{23}, \mathbf{x}_3, \mathbf{x}_{30}, \mathbf{x}_{20}. \end{aligned}$$

To match the above one non-zero value, similar to (21), we can get a  $\mathbf{u}_{h,5}$  supported on  $T_2$  and  $T_3$ . Define

$$p_{2,5} = p_{2,4} - \operatorname{div} \mathbf{u}_{h,5} \in L_0^2(Q) \cap P_h.$$

We have

$$\begin{aligned} p_{2,5}|_{T_2} &= 0, \\ p_{2,5}|_{T_3}(\mathbf{n}_0) &= p_{2,3}|_{T_3}(\mathbf{n}_0) - p_{2,3}|_{T_2}(\mathbf{n}_0) + p_{2,3}|_{T_1}(\mathbf{n}_0), \\ p_{2,5}|_{T_3}(\mathbf{y}) &= 0, \quad \mathbf{y} = \mathbf{x}_3, \mathbf{x}_{34}, \mathbf{x}_4, \mathbf{x}_{40}, \mathbf{x}_{30}. \end{aligned}$$



Repeating (21) one more time, we can get a  $\mathbf{u}_{h,6}$  supported on  $T_3$  and  $T_4$ . Define

$$p_{2,6} = p_{2,5} - \operatorname{div} \mathbf{u}_{h,6} \in L_0^2(Q) \cap P_h.$$

We have

$$\begin{cases} p_{2,6}|_{T_3} = 0, \\ p_{2,6}|_{T_4}(\mathbf{n}_0)a = p_{2,3}|_{T_4}(\mathbf{n}_0) - p_{2,3}|_{T_3}(\mathbf{n}_0) + p_{2,3}|_{T_2}(\mathbf{n}_0) - p_{2,3}|_{T_1}(\mathbf{n}_0), \\ p_{2,6}|_{T_4}(\mathbf{y}) = 0, \quad \mathbf{y} = \mathbf{x}_4, \mathbf{x}_{41}, \mathbf{x}_1, \mathbf{x}_{10}, \mathbf{x}_{40}. \end{cases} \quad (22)$$

Because  $p_{2,3} \in P_h$ , we do have

$$\sum_{i=1}^4 (-1)^i p_{2,3}|_{T_i}(\mathbf{n}_0) = 0.$$

By (22)

$$p_{2,6} = 0 \text{ on } T_i, \quad i = 1, 2, 3, 4.$$

Let  $\mathbf{u}_{h,i}$  be defined on all quadrilaterals as it is defined on this  $Q$ . Let

$$\mathbf{u}_h = \mathbf{u}_{h,1} + \mathbf{u}_{h,2} + \mathbf{u}_{h,3} + \mathbf{u}_{h,4} + \mathbf{u}_{h,5} + \mathbf{u}_{h,6}.$$

Then

$$\operatorname{div} \mathbf{u}_h = p_2.$$

As all the construction of late  $\mathbf{u}_{h,i}$  ( $i > 1$ ) is local, we have a uniform stability under corresponding norms. Thus

$$|\mathbf{u}_h|_1 \leq C \|p_2\|_0.$$

The lemma is proved.

### 3 Convergence

**Lemma 2** *The linear system of finite element equations (3)–(4) has a unique solution  $(\mathbf{u}_h, p_h) \in \mathbf{V}_h \times P_h$ , where  $\mathbf{V}_h$  and  $P_h$  are defined in (5) and (6), respectively.*

**Proof** For a finite square system of linear equations, we only need to prove the uniqueness. Let  $\mathbf{f} = \mathbf{0}$  in (3). Letting  $\mathbf{v}_h = \mathbf{u}_h$  in (3) and  $q_h = p_h$  in (4), we add the two equations to get

$$\|\nabla \mathbf{u}_h\|_0^2 = 0.$$

$\mathbf{u}_h$  would be constant vectors on each  $T$ . Because  $\mathbf{u}_h$  is continuous and it has a zero boundary condition,  $\mathbf{u}_h = \mathbf{0}$ . By the inf-sup condition (7) and (3), we have a  $\mathbf{v}_h$  such that  $\operatorname{div} \mathbf{v}_h = p_h$  and

$$\|p_h\|_0^2 = (\operatorname{div} \mathbf{v}_h, p_h) = 0,$$

which shows  $p_h = 0$ . The lemma is proved.

**Theorem 1** Let  $(\mathbf{u}, p) \in (H^4(\Omega) \cap H_0^1(\Omega))^2 \times (H^3(\Omega) \cap L_0^2(\Omega))$  be the solution of the stationary Stokes problem (1)–(2). Let  $(\mathbf{u}_h, p_h) \in \mathbf{V}_h \times P_h$  be the solution of the finite element problem (3)–(4). It holds that

$$\|\mathbf{u} - \mathbf{u}_h\|_1 \leq Ch^3 |\mathbf{u}|_4, \tag{23}$$

where  $C$  is independent of  $\mu$ .

**Proof** Subtracting (3) from (1), we get

$$(\nabla(\mathbf{u} - \mathbf{u}_h), \nabla \mathbf{v}_h) - (p - p_h, \operatorname{div} \mathbf{v}_h) = 0, \quad \forall \mathbf{v}_h \in \mathbf{V}_h, \tag{24}$$

and

$$(\nabla(\mathbf{u} - \mathbf{u}_h), \nabla \mathbf{z}_h) = 0, \quad \forall \mathbf{z}_h \in \mathbf{Z}_h, \tag{25}$$

where

$$\mathbf{Z}_h = \{\mathbf{z}_h \in \mathbf{V}_h : \operatorname{div} \mathbf{z}_h = 0\}.$$

By (25),

$$|\mathbf{u} - \mathbf{u}_h|_1^2 = (\nabla(\mathbf{u} - \mathbf{u}_h), \nabla(\mathbf{u} - \mathbf{z}_h)) \leq |\mathbf{u} - \mathbf{u}_h|_1 |\mathbf{u} - \mathbf{z}_h|_1.$$

That is,

$$|\mathbf{u} - \mathbf{u}_h|_1 = \inf_{\mathbf{z}_h \in \mathbf{Z}_h} |\mathbf{u} - \mathbf{z}_h|_1. \tag{26}$$

Let

$$\mathbf{Z}_h^\perp = \{\mathbf{v}_h \in \mathbf{V}_h : (\nabla \mathbf{v}_h, \nabla \mathbf{z}_h) = 0, \forall \mathbf{z}_h \in \mathbf{Z}_h\}.$$

For any  $\mathbf{v}_h \in \mathbf{V}_h$ , let  $\mathbf{y}_h \in \mathbf{Z}_h^\perp$  be the unique solution of

$$(\operatorname{div} \mathbf{y}_h, q_h) = (\operatorname{div}(\mathbf{u} - \mathbf{v}_h), q_h) = (-\operatorname{div} \mathbf{v}_h, q_h), \quad \forall q_h \in P_h. \tag{27}$$

By the on-to condition (7) and the inf-sup condition (8), we have  $\operatorname{div} \mathbf{V}_h = P_h$  and (27) has solutions. All such solutions are projected to the unique solution in  $\mathbf{Z}_h^\perp$ . Letting  $q_h = -\operatorname{div} \mathbf{v}_h$  in (27), we get

$$\|\operatorname{div} \mathbf{v}_h\|_0^2 = (\operatorname{div} \mathbf{y}_h, q_h) \geq \beta |\mathbf{y}_h|_1 \|q_h\|_0.$$

Thus

$$|\mathbf{y}_h|_1 \leq \beta^{-1} \|q_h\|_0 = \beta^{-1} \|\operatorname{div}(\mathbf{u} - \mathbf{v}_h)\|_0 \leq \beta^{-1} |\mathbf{u} - \mathbf{v}_h|_1,$$

and

$$\operatorname{div}(\mathbf{v}_h + \mathbf{y}_h) = 0, \text{ i.e., } \mathbf{v}_h + \mathbf{y}_h \in \mathbf{Z}_h.$$

By (26), we have

$$\begin{aligned}
 |\mathbf{u} - \mathbf{u}_h|_1 &= \inf_{\mathbf{z}_h \in \mathbf{Z}_h} |\mathbf{u} - \mathbf{z}_h|_1 \leq \inf_{\mathbf{v}_h \in \mathbf{V}_h} |\mathbf{u} - (\mathbf{v}_h + \mathbf{y}_h)|_1 \\
 &\leq \inf_{\mathbf{v}_h \in \mathbf{V}_h} |\mathbf{u} - \mathbf{v}_h|_1 + |\mathbf{y}_h|_1 \\
 &\leq (1 + \beta^{-1}) \inf_{\mathbf{v}_h \in \mathbf{V}_h} |\mathbf{u} - \mathbf{v}_h|_1 \\
 &\leq (1 + \beta^{-1}) |\mathbf{u} - \mathbf{I}_h \mathbf{u}|_1 \\
 &\leq Ch^3 |\mathbf{u}|_4,
 \end{aligned}$$

where  $\mathbf{I}_h$  is the nodal interpolation operator defined by DOF of (5). As  $\mathbf{V}_h$  includes all  $P_3$  polynomials, such an  $\mathbf{I}_h$  can be proved  $H^1$ -stable and quasi-optimal up to order 3 in  $H^1$ -norm, cf. [18]. The proof is complete.

**Theorem 2** Let  $(\mathbf{u}, p) \in (H^4(\Omega) \cap H_0^1(\Omega))^2 \times (H^3(\Omega) \cap L_0^2(\Omega))$  be the solution of the stationary Stokes problem (1)–(2). Let  $(\mathbf{u}_h, p_h) \in \mathbf{V}_h \times P_h$  be the solution of the finite element problem (3)–(4). It holds that

$$\|p - p_h\|_0 \leq Ch^3 (\mu |\mathbf{u}|_4 + |p|_3). \tag{28}$$

**Proof** By (24) and (8), we get

$$\begin{aligned}
 \beta |\mathbf{v}_h| \| \Pi_h p - p_h \| &\leq |(\operatorname{div} \mathbf{v}_h, \Pi_h p - p_h)| \\
 &= |(\operatorname{div} \mathbf{v}_h, p - p_h)| = |(\mu \nabla(\mathbf{u} - \mathbf{u}_h), \nabla \mathbf{v}_h)| \\
 &\leq \mu |\mathbf{u} - \mathbf{u}_h|_1 |\mathbf{v}_h|_1,
 \end{aligned}$$

where  $\Pi_h$  is the  $L^2$  projection operator onto  $P_h$ . Hence,

$$\begin{aligned}
 \|p - p_h\|_0 &\leq \|p - \Pi_h p\|_0 + \beta^{-1} |\mathbf{u} - \mathbf{u}_h|_1 \\
 &\leq Ch^3 (|p|_3 + \mu |\mathbf{u}|_4).
 \end{aligned}$$

Thus, (28) is proved.

**Theorem 3** Let  $(\mathbf{u}, p) \in (H^4(\Omega) \cap H_0^1(\Omega))^2 \times (H^3(\Omega) \cap L_0^2(\Omega))$  be the solution of the stationary Stokes problem (1)–(2). Let  $(\mathbf{u}_h, p_h) \in \mathbf{V}_h \times P_h$  be the solution of the finite element problem (3)–(4). It holds that

$$\|\mathbf{u} - \mathbf{u}_h\|_0 \leq Ch^4 |\mathbf{u}|_4, \tag{29}$$

where  $C$  is independent of  $\mu$ .

**Proof** We will use the duality argument. Let  $\mathbf{w} \in H_0^1(\Omega)^2$  and  $r \in L_0^2(\Omega)$  such that

$$-\operatorname{div}(\mu \nabla \mathbf{w}) + \nabla r = \mathbf{u} - \mathbf{u}_h \quad \text{in } \Omega, \tag{30}$$

$$\operatorname{div} \mathbf{w} = 0 \quad \text{in } \Omega. \tag{31}$$

We assume the following regularity:

$$\mu |\mathbf{w}|_2 + |r|_1 \leq C \|\mathbf{u} - \mathbf{u}_h\|_0. \tag{32}$$

Multiplying (30) by  $(\mathbf{u} - \mathbf{u}_h)$  and doing integration by parts, we get

$$(\mu \mathbf{u} - \mathbf{u}_h, \mathbf{u} - \mathbf{u}_h) = (\mu \nabla \mathbf{w}, \nabla(\mathbf{u} - \mathbf{u}_h)) - (\operatorname{div}(\mathbf{u} - \mathbf{u}_h), r). \tag{33}$$

Let  $\mathbf{w}_h \in \mathbf{V}_h$  and  $r_h \in P_h$  be the finite element solution for problem (30)–(31), satisfying

$$(\mu \nabla \mathbf{w}_h, \nabla \mathbf{v}_h) - (\operatorname{div} \mathbf{v}_h, r_h) = (\mathbf{u} - \mathbf{u}_h, \mathbf{v}_h), \quad \forall \mathbf{v}_h \in \mathbf{V}_h, \tag{34}$$

$$(\operatorname{div} \mathbf{w}_h, q_h) = 0, \quad \forall q_h \in P_h. \tag{35}$$

Letting  $\mathbf{v}_h = \mathbf{w}_h$  in (24), we get

$$(\mu \nabla(\mathbf{u} - \mathbf{u}_h), \nabla \mathbf{w}_h) = (\operatorname{div} \mathbf{w}_h, \Pi_h p - p_h) = 0. \tag{36}$$

Subtracting (36) from (33), we get

$$\mu \|\mathbf{u} - \mathbf{u}_h\|_0^2 = (\mu \nabla(\mathbf{w} - \mathbf{w}_h), \nabla(\mathbf{u} - \mathbf{u}_h)) - (\operatorname{div}(\mathbf{u} - \mathbf{u}_h), r - \Pi_h r). \tag{37}$$

We have, by the quasi-optimal error bound (23) and the assumed elliptic regularity (32), from (37),

$$\begin{aligned} \|\mathbf{u} - \mathbf{u}_h\|_0^2 &\leq \mu \|\nabla(\mathbf{w} - \mathbf{w}_h)\|_0 \|\nabla(\mathbf{u} - \mathbf{u}_h)\|_0 + \|\mathbf{u} - \mathbf{u}_h\|_1 \|r - \Pi_h r\|_0 \\ &\leq Ch^4 |\mathbf{u}|_4 (\mu |\mathbf{w}|_2 + |r|_1) \\ &\leq Ch^4 |\mathbf{u}|_4 \|\mathbf{u} - \mathbf{u}_h\|_0. \end{aligned} \tag{38}$$

Thus, (29) follows (38).

### 4 Numerical Experiments

In the numerical computation, the domain is  $\Omega = (0, 1) \times (0, 1)$ . We choose an  $\mathbf{f}$  in (1) so that the exact solution is

$$\begin{cases} \mathbf{u} = \begin{pmatrix} -2^7(x-x^2)^2(y-y^2)(1-2y) \\ 2^7(x-x^2)(1-2x)(y-y^2)^2 \end{pmatrix}, \\ p = x - \frac{1}{2}. \end{cases} \tag{39}$$

We compute the solution (39) on the uniform triangular grids shown in Fig. 3, by the divergence-free  $P_3$ - $P_2$  finite element and the Taylor-Hood  $P_3$ - $P_2$  finite element. The results are listed in Tables 1 and 2. We can see that the optimal order of convergence is achieved in all cases for the two finite elements in Tables 1 and 2. Both methods have the same numbers of unknowns for the velocity. The divergence-free  $P_3$ - $P_2$  method has more pressure unknowns than the Taylor-Hood  $P_3$ - $P_2$  method. However, from Table 1, all errors of the Taylor-Hood  $P_3$ - $P_2$  method are smaller, when  $\mu = 1$ .

We can see, from Table 1, that the divergence-free  $P_3$ - $P_2$  method performs worse than the Taylor-Hood  $P_3$ - $P_2$  method, when  $\mu = 1$ . But it shows the opposite in Table 2 when  $\mu = 10^{-8}$ . Both the velocity error and the pressure error of the Taylor-Hood  $P_3$ - $P_2$  element

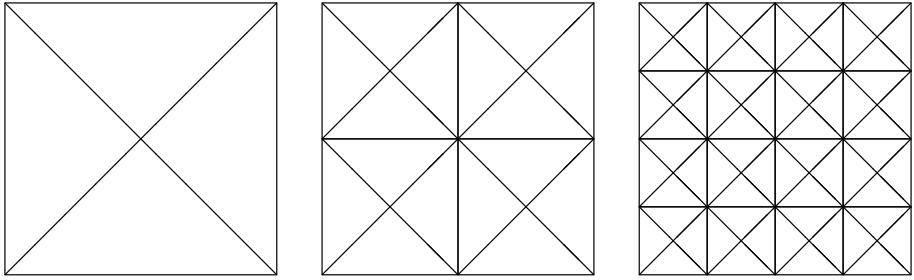


Fig. 3 The first three levels of grids for the computation in Tables 1 and 2

Table 1 Error profile on the triangular meshes shown as in Fig. 3 for the solution (39),  $\mu = 1$

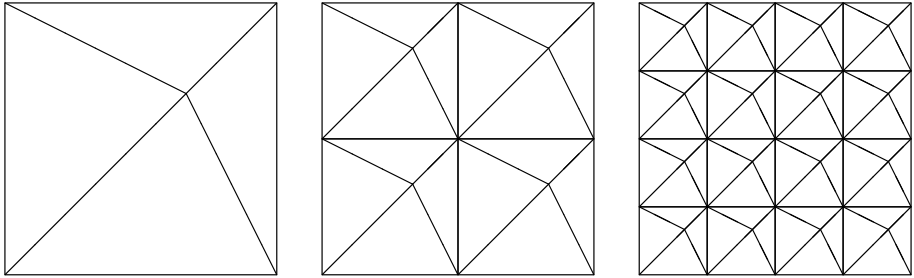
Grid	$\ \mathbf{u} - \mathbf{u}_h\ _0$	$O(h^r)$	$\ \mathbf{u} - \mathbf{u}_h\ _1$	$O(h^r)$	$\ \Pi_h p - p_h\ _0$	$O(h^r)$
By the divergence-free $P_3$ - $P_2$ element, $\mu = 1$						
3	0.673 6E-03	4.1	0.318 0E-01	3.0	0.146 5E+00	3.4
4	0.404 0E-04	4.1	0.386 1E-02	3.0	0.130 2E-01	3.5
5	0.244 3E-05	4.0	0.475 9E-03	3.0	0.135 0E-02	3.3
By the Taylor-Hood $P_3$ - $P_2$ element, $\mu = 1$						
3	0.263 3E-03	3.5	0.127 4E-01	2.7	0.897 4E-02	2.8
4	0.169 9E-04	4.0	0.159 6E-02	3.0	0.104 0E-02	3.1
5	0.106 4E-05	4.0	0.195 7E-03	3.0	0.109 5E-03	3.2

Table 2 Error profile on the triangular meshes shown as in Fig. 3 for the solution (39),  $\mu = 10^{-8}$

Grid	$\ \mathbf{u} - \mathbf{u}_h\ _0$	$O(h^r)$	$\ \mathbf{u} - \mathbf{u}_h\ _1$	$O(h^r)$	$\ \Pi_h p - p_h\ _0$	$O(h^r)$
By the divergence-free $P_3$ - $P_2$ element, $\mu = 10^{-8}$						
3	0.673 6E-03	4.1	0.318 0E-01	3.0	0.149 6E-08	3.4
4	0.404 0E-04	4.1	0.386 1E-02	3.0	0.148 4E-09	3.3
5	0.244 4E-05	4.0	0.475 9E-03	3.0	0.474 7E-11	5.0
By the Taylor-Hood $P_3$ - $P_2$ element, $\mu = 10^{-8}$						
3	0.321 3E+03	3.4	0.133 4E+01	2.6	0.122 7E-03	3.4
4	0.233 5E+02	3.8	0.187 3E+00	2.8	0.122 8E-04	3.3
5	0.155 9E+01	3.9	0.246 9E-01	2.9	0.132 8E-05	3.2

are about  $10^6$  times larger than the corresponding error of the divergence-free  $P_3$ - $P_2$  element. In fact, the discrete velocity  $\mathbf{u}_h$  remains same, from Tables 1 and 2, when  $\mu$  changes, verifying our theory that the  $\mathbf{u}_h$  convergence is independent of  $\mu$ .

Next, we compute the above example again, but on perturbed meshes, shown in Fig. 4, by the divergence-free  $P_3$ - $P_2$  element and the Taylor-Hood  $P_3$ - $P_2$  element. All comments made above on Tables 1 and 2 remain same for Tables 3 and 4. Between the errors on Fig. 3 meshes and on Fig. 4 meshes, the latter ones are about double the earlier ones. It is always true that it works better on meshes with the singular vertex.



**Fig. 4** The first three levels of grids for the computation in Tables 3 and 4

**Table 3** Error profile on the triangular meshes shown as in Fig. 4 for the solution (39),  $\mu = 1$

Grid	$\ \mathbf{u} - \mathbf{u}_h\ _0$	$O(h^r)$	$ \mathbf{u} - \mathbf{u}_h _1$	$O(h^r)$	$\ \Pi_h p - p_h\ _0$	$O(h^r)$
By the divergence-free $P_3$ - $P_2$ element, $\mu = 1$						
3	0.165 2E-02	3.8	0.688 9E-01	2.8	0.397 6E+00	2.9
4	0.971 8E-04	4.1	0.815 5E-02	3.1	0.429 1E-01	3.2
5	0.561 5E-05	4.1	0.957 9E-03	3.1	0.460 5E-02	3.2
By the Taylor-Hood $P_3$ - $P_2$ element, $\mu = 1$						
3	0.403 8E-03	3.6	0.165 9E-01	2.6	0.183 3E-01	2.8
4	0.268 2E-04	3.9	0.218 8E-02	2.9	0.217 0E-02	3.1
5	0.169 7E-05	4.0	0.274 5E-03	3.0	0.236 6E-03	3.2

**Table 4** Error profile on the triangular meshes shown as in Fig. 4 for the solution (39),  $\mu = 10^{-8}$

Grid	$\ \mathbf{u} - \mathbf{u}_h\ _0$	$O(h^r)$	$ \mathbf{u} - \mathbf{u}_h _1$	$O(h^r)$	$\ \Pi_h p - p_h\ _0$	$O(h^r)$
By the divergence-free $P_3$ - $P_2$ element, $\mu = 10^{-8}$						
3	0.165 2E-02	3.8	0.688 9E-01	2.8	0.400 3E-08	2.9
4	0.971 8E-04	4.1	0.815 5E-02	3.1	0.526 6E-09	2.9
5	0.561 5E-05	4.1	0.957 9E-03	3.1	0.113 4E-10	5.5
By the Taylor-Hood $P_3$ - $P_2$ element, $\mu = 10^{-8}$						
3	0.311 7E+01	3.4	0.133 3E+00	2.6	0.138 9E-03	3.3
4	0.226 2E+00	3.8	0.186 8E-01	2.8	0.148 0E-04	3.2
5	0.151 0E-01	3.9	0.246 0E-02	2.9	0.169 0E-05	3.1

**Author Contributions** The single author made all contribution.

**Declarations**

**Conflict of Interest** There is no potential conflict of interest.

**Compliance with Ethical Standards** The submitted work is original and is not published elsewhere in any form or language.

**Ethical Approval** This article does not contain any studies involving animals. This article does not contain any studies involving human participants.

**Informed Consent** This research does not have any human participant.

## References

1. Arnold, D. N., Qin, J.: Quadratic velocity/linear pressure Stokes elements. In: Vichnevetsky, R., Steplemen, R.S. (eds.) *Advances in Computer Methods for Partial Differential Equations VII* (1992)
2. Fabien, M., Guzman, J., Neilan, M., Zytoon, A.: Low-order divergence-free approximations for the Stokes problem on Worsley-Farin and Powell-Sabin splits. *Comput. Methods Appl. Mech. Eng.* **390**, 21 (2022). (Paper No. 114444)
3. Falk, R., Neilan, M.: Stokes complexes and the construction of stable finite elements with pointwise mass conservation. *SIAM J. Numer. Anal.* **51**(2), 1308–1326 (2013)
4. Guzman, J., Neilan, M.: Conforming and divergence-free Stokes elements on general triangular meshes. *Math. Comput.* **83**(285), 15–36 (2014)
5. Guzman, J., Neilan, M.: Conforming and divergence-free Stokes elements in three dimensions. *IMA J. Numer. Anal.* **34**(4), 1489–1508 (2014)
6. Guzman, J., Neilan, M.: Inf-sup stable finite elements on barycentric refinements producing divergence-free approximations in arbitrary dimensions. *SIAM J. Numer. Anal.* **56**(5), 2826–2844 (2018)
7. Huang, J., Zhang, S.: A divergence-free finite element method for a type of 3D Maxwell equations. *Appl. Numer. Math.* **62**(6), 802–813 (2012)
8. Huang, Y., Zhang, S.: A lowest order divergence-free finite element on rectangular grids. *Front. Math. China* **6**(2), 253–270 (2011)
9. Huang, Y., Zhang, S.: Supercloseness of the divergence-free finite element solutions on rectangular grids. *Commun. Math. Stat.* **1**(2), 143–162 (2013)
10. Kean, K., Neilan, M., Schneier, M.: The Scott-Vogelius method for the Stokes problem on anisotropic meshes. *Int. J. Numer. Anal. Model.* **19**(2/3), 157–174 (2022)
11. Neilan, M.: Discrete and conforming smooth de Rham complexes in three dimensions. *Math. Comput.* **84**(295), 2059–2081 (2015)
12. Neilan, M., Otus, B.: Divergence-free Scott-Vogelius elements on curved domains. *SIAM J. Numer. Anal.* **59**(2), 1090–1116 (2021)
13. Neilan, M., Sap, D.: Stokes elements on cubic meshes yielding divergence-free approximations. *Calcolo* **53**(3), 263–283 (2016)
14. Qin, J.: On the convergence of some low order mixed finite elements for incompressible fluids. Thesis. Pennsylvania State University (1994)
15. Qin, J., Zhang, S.: Stability and approximability of the  $P_1$ - $P_0$  element for Stokes equations. *Int. J. Numer. Methods Fluids* **54**, 497–515 (2007)
16. Scott, L.R., Vogelius, M.: Norm estimates for a maximal right inverse of the divergence operator in spaces of piecewise polynomials. *RAIRO Model. Math. Anal. Numer.* **19**, 111–143 (1985)
17. Scott, L.R., Vogelius, M.: Conforming Finite Element Methods for Incompressible and Nearly Incompressible Continua. In: *Lectures in Appl. Math.*, vol. 22, pp. 221–244 (1985)
18. Scott, L.R., Zhang, S.: Higher-dimensional nonnested multigrid methods. *Math. Comput.* **58**(198), 457–466 (1992)
19. Xu, X., Zhang, S.: A new divergence-free interpolation operator with applications to the Darcy-Stokes-Brinkman equations. *SIAM J. Sci. Comput.* **32**(2), 855–874 (2010)
20. Ye, X., Zhang, S.: A numerical scheme with divergence free H-div triangular finite element for the Stokes equations. *Appl. Numer. Math.* **167**, 211–217 (2021)
21. Zhang, S.: A new family of stable mixed finite elements for 3D Stokes equations. *Math. Comput.* **74**(250), 543–554 (2005)
22. Zhang, S.: On the  $P_1$  Powell-Sabin divergence-free finite element for the Stokes equations. *J. Comput. Math.* **26**, 456–470 (2008)
23. Zhang, S.: A family of  $Q_k + 1, k \times Q_k, k + 1$  divergence-free finite elements on rectangular grids. *SIAM J. Numer. Anal.* **47**, 2090–2107 (2009)
24. Zhang, S.: Quadratic divergence-free finite elements on Powell-Sabin tetrahedral grids. *Calcolo* **48**(3), 211–244 (2011)

25. Zhang, S.: Divergence-free finite elements on tetrahedral grids for  $k \geq 6$ . *Math. Comput.* **80**, 669–695 (2011)
26. Zhang, S.: A P4 bubble enriched P3 divergence-free finite element on triangular grids. *Comput. Math. Appl.* **74**(11), 2710–2722 (2017)

Springer Nature or its licensor (e.g. a society or other partner) holds exclusive rights to this article under a publishing agreement with the author(s) or other rightsholder(s); author self-archiving of the accepted manuscript version of this article is solely governed by the terms of such publishing agreement and applicable law.